Bulletin of Mathematical Biology (2002) **64**, 327–353
doi:10.1006/bulm.2001.0277
Available online at http://www.idealibrary.com on IDEAL®

Modelling *Dictyostelium discoideum* Morphogenesis: the Culmination

ATHANASIUS F. M. MARÉE* AND PAULIEN HOGEWEG
Theoretical Biology and Bioinformatics,
University of Utrecht,
Padualaan 8,
3584 CH Utrecht,
The Netherlands

The culmination of the morphogenesis of the cellular slime mould *Dictyostelium discoideum* involves complex cell movements which transform a mound of cells into a globule of spores on a slender stalk. We show that cyclic AMP signalling and differential adhesion, combined with cell differentiation and slime production, are sufficient to produce the morphogenetic cell movements which lead to culmination. We have simulated the process of culmination using a hybrid cellular automata/-partial differential equation model. With our model we have been able to reproduce the main features that occur during culmination, namely the straight downward elongation of the stalk, its anchoring to the substratum and the formation of the long thin stalk topped by the spore head.
We conclude that the cyclic AMP signalling system is responsible for the elongation and anchoring of the stalk, but in a roundabout way: pressure waves that are induced by the chemotaxis towards cyclic AMP squeeze the stalk through the cell mass. This mechanism forces the stalk to elongate precisely in the direction opposite to that of the chemotactically moving cells. The process turns out to be 'guided' by inactive 'pathfinder' cells, which form the tip of the stalk. We show that the entire development is enacted by means of the aforementioned building blocks. This means that no global gradients or different modes of chemotaxis are needed to complete the culmination.
MPEG movies of the simulations are available on-line: `http://www-binf.bio.uu.nl/stan/bmb`.

1. INTRODUCTION

When their bacterial food source is depleted individual amoebae of the cellular slime mould *Dictyostelium discoideum* aggregate to form a multicellular migratory slug, which is surrounded by a slime sheath. The slug has phototactic and thermotactic properties, which direct it to a suitable site for culmination. When

*Author to whom correspondence should be addressed. Current address: Department of Mathematics, University of British Columbia, Vancouver, BC, Canada V6T 1Z2.
E-mail: stan@iam.ubc.ca

0092-8240/02/020327 + 27 $35.00/0

conditions are right, migration halts and in about 4 h a fruiting body is formed; the fruiting body has a stalk that supports a spore head elevated above the substratum to facilitate spore dispersal.

Our theoretical understanding of *Dictyostelium* morphogenesis is progressing in the same way as the morphogenesis itself. Initially, the focus was mainly on the aggregation (Keller and Segel, 1970; Nanjundiah, 1973; Parnas and Segel, 1977; Tyson and Murray, 1989) and stream formation (MacKay, 1978; Levine and Reynolds, 1991; Vasiev *et al*., 1994; Höfer *et al*., 1995; Van Oss *et al*., 1996); more recently the mound formation and slug migration have been studied (Bretschneider *et al*., 1995; Savill and Hogeweg, 1997; Dormann *et al*., 1998; Jiang *et al*., 1998; Bretschneider *et al*., 1999; Marée *et al*., 1999a,b; Vasiev and Weijer, 1999; Palsson and Othmer, 2000). So far, however, the culmination stage has received little attention.

In this paper we specifically analyse the complex cell movements that lead to the formation of the fruiting body. The processes that are incorporated in our model to describe the culmination are basically the same as those that dominate the earlier stages of the development, from aggregation onwards. These processes are cyclic AMP (cAMP) signalling and cell adhesion between a small number of differentiating cell types. The dynamics observed during culmination involve stalk formation, cell movement and cell differentiation. We will describe what is known about these processes as a result of experiments.

The principal results of this paper were briefly presented in Marée and Hogeweg (2001). The present paper contains additional important material concerning several major issues.

1.1. ***Stalk formation.*** It is beyond the scope of this paper to review the origin of many of the relevant observations made by previous workers; we mention only those papers that are of immediate pertinence. For a comprehensive review of the earlier work, see Kessin (2001).

Very early during morphogenesis the amoebae are differentiated into two main cell types, prestalk and prespore cells. At the start of culmination the prestalk cells occupy the upper 30% of the culminant, while the prespore cells occupy the lower part.

The movement during culmination has been likened to a ‘reverse fountain’, whereby the prestalk cells in the upper part form a stalk that moves downwards to anchor itself to the base, while the prespore cells from the lower part move upwards to form the spore head. The stalk moves remarkably fast through the centre of the cell mass: Sternfeld (1992) found that the tip of the stalk reached the base only about 20 min after penetrating the prespore region. Higuchi and Yamada (1984) found that the movement took only 11 min. When the stalk tip becomes anchored to the substratum, it becomes slightly thickened (Higuchi and Yamada, 1984). No lateral motion of the stalk has been observed.

The stalk is surrounded by an extracellular matrix, called the stalk tube. The major component of the stalk tube is cellulose. Its composition differs from that of the surface slime sheath in that it is much more rigid (Jermyn and Williams, 1991; Grimson *et al*., 1996). At the top of the stalk tube a funnel-shaped gate is formed, through which the prestalk cells enter the tube. Also at the apex the tube is extended by the addition of tube material (Kessin, 2001). Cells that have just entered the tube and are differentiating into stalk cells excrete tube material: EcmB, a stalk cell-specific protein, forms part of the stalk tube (Williams *et al*., 1993); and when the differentiation into stalk cells is blocked, production of tube material seems to cease (Amagai *et al*., 1983). However, prestalk cells that move up on the outside of the tube also deposit additional tube material prior to entering the tube (Bonner *et al*., 1955; Blanton, 1997).

The tip of the stalk is surrounded by a cluster of cells. These cells are believed to guide the straight downward motion of the stalk. Hence they are called 'pathfinder' or 'vanguard' cells (Jermyn and Williams, 1991). The culminant also forms a basal disc, which gives the organism its scientific name, and an upper and lower cup, which surround the rising spore mass.

Gravity plays a minor role in stalk formation. Counter-intuitively, stalk length becomes slightly shorter when gravity decreases, but there is no difference between positively or negatively directed gravity (Kawasaki *et al*., 1990). Normally, the stalk becomes positioned perpendicular to the substratum, independent of the orientation of the substratum with respect to the gravitational field. However, ammonia (NH_3) influences the process of culmination: culminants orient away from NH_3 (Bonner *et al*., 1986), as well as away from each other, presumably also due to NH_3 production (Feit and Sollitto, 1987).

1.2. ***Cell differentiation.*** The prestalk cells can be divided into prestalk O (PstO) cells, prestalk A (PstA) cells and prestalk AB (PstAB) cells. The PstAB cells form the upper part of the stalk, the PstA cells occupy the top 10% of the culminant, and the PstO cells occupy the lower part of the prestalk-zone. During culmination a unidirectional conversion of cell types takes place: PstO cells differentiate into PstA cells, and PstA cells into PstAB cells (Williams *et al*., 1989; Sternfeld, 1992). Whereas the transition of PstO into PstA cells takes place slowly and gradually, differentiation of PstA into PstAB is very rapid, and happens only when PstA cells enter the stalk tube: the cells do not express the PstAB-specific marker until they are just inside the entrance (Jermyn and Williams, 1991). The PstAB cells rapidly differentiate into mature stalk cells, deposit cellulose and die (Whittingham and Raper, 1960). During this process, the cells become vacuolated, which leads to a significant volume increase (Williams *et al*., 1989; Sternfeld, 1992).

However, a special group of PstAB cells develop during the slug stage. During this stage they are located in the central core at the front. These PstAB cells, which are initially present in the tip of the migrating slug, later on form the tip of the downward moving stalk, i.e., they form the aforementioned cluster of pathfinder

cells. The remainder of the stalk consists of PstAB cells that are recruited only later, during the culmination stage. Hence the pathfinder cells are sometimes also called 'early stalk cells'. Pathfinder cells look like immature stalk cells, with little cytoplasm and a large central vacuole, but apparently they do not produce tube material (Jermyn and Williams, 1991; Sternfeld, 1992; Jermyn *et al*., 1996).

1.3. ***Cell movements.*** During culmination complex cell movements are observed. The cAMP plays a central role in the regulation of cell motion in *Dictyostelium*. There seems to be increasing evidence that cAMP signalling continues after aggregation is complete and organizes cell movement during both slug migration and fruiting body formation (Siegert and Weijer, 1992, 1995; Verkerke-Van Wijk and Schaap, 1997; Dormann *et al*., 1998; Weijer, 1999; Dormann *et al*., 2000). The overview papers on the work done by Weijer and colleagues, especially, offer compelling evidence that the process of cAMP signalling and chemotactic cell movement continues during the whole morphogenesis (Weijer, 1999; Dormann *et al*., 2000). Such coordinated cell movement is organized by a combination of a pulsatile cAMP excretion and a cAMP-mediated cAMP response, accompanied by a chemotactic response towards the cAMP. Because of their high-frequency pulsatile cAMP excretion, PstA cells are considered to be the source of the cAMP waves (Kitami, 1984).

However, there is, as yet, no clue as to the stimulus that directs the downward movement of the stalk and pathfinder cells (Williams, 1997). Stalk cells neither excrete cAMP nor exhibit negative chemotaxis away from cAMP. The pathfinder cells do not seem to respond to cAMP either: during the slug stage they often disappear in the slime trail in the case of prolonged migration (Sternfeld, 1992). Nonetheless, the symmetry in upward and downward motion is striking (Williams, 1997). It seems unlikely that the pathfinder cells are able to transport the whole stalk downwards, and it also seems unrealistic to assume that the stalk cells themselves move, for they lose their motility very quickly after entering the stalk tube and die after a relatively short period of time (Watts and Treffry, 1976). Therefore it is generally assumed that the tip elongates due to the addition of stalk cells at the tube mouth (Jermyn and Williams, 1991; Thomason *et al*., 1999).

Not only cAMP, but also cell–cell adhesion and cell–substratum adhesion play an important role in regulating cell movements. Besides, adhesion plays a role in many other processes during all stages of the development, such as cohesion, cell sorting (a process that has been recently challenged by Clow *et al*., 2000), and contact-mediated regulation of gene expression. Hence in many respects adhesion is essential for normal development (Fontana, 1995; Bozzaro and Ponte, 1995).

In this study we show that the following elements are sufficient to produce all the dynamics observed during the culmination: cAMP signalling, differential adhesion, cell differentiation and extracellular matrices. We show how a stalk surrounded by a tube is formed, how its fast and straight downward motion through

the cell mass takes place, without the need for any other chemical or other mode of chemotaxis, and how eventually a globule of spores on a slender stalk develops.

2. THE MODEL

In the last few years several models have been devised to describe the mound and slug stage (see, e.g., Dormann *et al*., 1998; Jiang *et al*., 1998; Marée *et al*., 1999a,b; Bretschneider *et al*., 1999). However, the culmination stage has hardly been modelled at all. Although Zeeman (1977) and Rubinow *et al*. (1981) tried to catch the shape of the culminant in mathematical equations, no dynamical model based on biological processes has yet been formulated.

The model described in this paper incorporates cell differentiation by local induction processes, cell–cell and cell–substratum adhesion, cAMP signalling with chemotaxis towards cAMP, and production of tube material. We show how these local processes and their interactions are sufficient to produce the dynamics of the culmination stage.

All the building blocks mentioned earlier can be very elegantly combined to interact with each other by means of the two-scale cellular automata (CA) model-formalism developed by Glazier and Graner (1993), extended with an extra layer for partial differential equations (PDEs) (Savill and Hogeweg, 1997). In this hybrid formalism the CA model-formalism is used to represent individual cells. They are, however, represented as a group of connected automata; that is, the basic scale of the model is subcellular. The PDEs are used to describe the cAMP dynamics.

For simplicity we have modelled the culmination using two-dimensional (2D) simulations. The simulations are considered to be transverse sections. Hence we obtain side views of the culminant. In some cases a fruiting body is seen to develop from flattened quasi-2D slugs (Miura and Siegert, 2000), which provides extra support for such an approach. As our initial configuration we take the starting point of the final culmination, when the culminant forms a more or less hemispherical shape (Higuchi and Yamada, 1984).

2.1. ***Adhesion.*** In the model-formalism, cell–cell and cell–substratum adhesions are implemented as follows. Each cell has a unique identification number, σ, which is assigned to the about 30 automata in the CA which form the cell. Each cell also has a type label, τ, which indicates whether the cell type is prespore, PstO, PstA, stalk or pathfinder ($\tau \in$ {Psp, PstO, PstA, St, Pf}), i.e., PstAB and stalk cells are lumped together in one cell type. Each automaton that is part of a cell's boundary has a number of dimensionless free-energy bonds. The magnitude of these bonds depends on the types they connect. The energy bonds are given by $J_{\tau_1,\tau_2} > 0$. The bond energy between a certain type and the air is given by $J_{\tau,A}$, and between a

certain type and the substratum by $J_{\tau,S}$. The total free energy of a cell is given by:

$$H_\sigma = \sum \frac{J_{\text{type,type}}}{2} + \sum J_{\text{type,A}} + \sum J_{\text{type,S}} + \lambda(v - V)^2, \tag{1}$$

where v is the actual volume, V the target volume, and λ the inelasticity. The final term ensures that the volume of a cell remains close to V. Minimization of the free energy causes deformation of the boundaries: at every time step all CAs are chosen in a random sequence, and for each CA we calculate whether it will copy itself into a random neighbour. The probability of such a change in cell shape is determined by the change in free energy ΔH if the extension were to occur. The probability is either 1 if $\Delta H < -H_{\text{diss}}$, or $e^{-\left(\frac{\Delta H + H_{\text{diss}}}{T}\right)}$ if $\Delta H \geq -H_{\text{diss}}$. H_{diss} represents the dissipation costs involved in deforming a boundary, which are associated with every change in cell shape. T represents the default motility of the cells.

To describe the slime sheath and the stalk tube, two entities are defined which follow the same rules; these can deform in the same way as all cells but have a much larger target volume V, and hence model-wise can be regarded as being two very large cells. This means that the slime sheath and stalk tube have their own identification number σ and type label τ ($\tau \in$ {Sl, Tu}). The slime sheath has a fixed target volume. The target volume of the stalk tube however slowly increases due to the production of tube material by prestalk cells that move up on the outside of the tube and cells that have entered the tube and are differentiating into stalk cells. This is modelled by adding a fixed volume every time a new stalk cell appears. To describe the very stiff nature of the stalk tube, which we consider to be equivalent to the high effort required to deform its shape, we have considerably increased the dissipation costs (H_{tubediss}). Instead of varying the inelasticity λ to model such differences in stiffness, we decided to vary H_{diss}. We did this for two reasons: firstly, H_{diss} is the parameter which describes best what we consider to be 'stiffness', and secondly, the conservation of cells constrains the permissible λ-values.

The values for cell adhesion are given in Table 1. The choice and sensitivity of these parameters are discussed in the Results section. It is also useful to define surface tensions in terms of the bond energies J_{τ_1,τ_2} (Glazier and Graner, 1993). Surface tensions between cell types are defined as:

$$\gamma_{\tau_1,\tau_2} = J_{\tau_1,\tau_2} - \frac{J_{\tau_1,\tau_1} + J_{\tau_2,\tau_2}}{2}, \tag{2}$$

and surface tensions between a cell type and the air (and, likewise, between a cell type and the substratum) are defined as:

$$\gamma_{\tau,\text{A}} = J_{\tau,\text{A}} - \frac{1}{2} J_{\tau,\tau}. \tag{3}$$

The surface tensions are also given in Table 1.

Table 1. The values of the energy bonds J_{τ_1,τ_2} and surface tensions γ_{τ_1,τ_2}, the initial number of cells, their target volume, and the type of cAMP dynamics (cAMP relay, oscillatory or small decay) used in the simulations. The surface tensions were calculated using equations (2) and (3).

τ			$J_{\tau,\mathrm{Psp}}$	$J_{\tau,\mathrm{PstO}}$	$J_{\tau,\mathrm{PstA}}$	$J_{\tau,\mathrm{St}}$	$J_{\tau,\mathrm{Pf}}$	$J_{\tau,\mathrm{Sl}}$	$J_{\tau,\mathrm{Tu}}$	$J_{\tau,\mathrm{A}}$	$J_{\tau,\mathrm{S}}$	#cells	V	cAMP
Psp	15.5	6.5	9	13	13	25	10	8	10	20	11	1960	30	relay
PstO	23.5	10.5	5.0	7	10	24	10	15	11	27	14	1011	30	relay
PstA	31.5	14.5	7.0	5.0	3	16	17	21	12	33	16	79	30	oscill.
St	41.5	18.5	19.0	19.0	13.0	3	7	21	3	43	20	25	30–40	decay
Pf	29.5	2.5	0.0	1.0	10.0	0.0	11	7	5	35	8	14	30	decay
Sl	5.0	7.0	3.5	11.5	19.5	19.5	1.5	–	1	5	7	1	3000	decay
Tu	5.0	9.0	5.5	7.5	10.5	1.5	-0.5	1.0	–	5	9	1	3×#*St*	–
	$\gamma_{\tau,\mathrm{A}}$	$\gamma_{\tau,\mathrm{S}}$	$\gamma_{\tau,\mathrm{Psp}}$	$\gamma_{\tau,\mathrm{PstO}}$	$\gamma_{\tau,\mathrm{PstA}}$	$\gamma_{\tau,\mathrm{St}}$	$\gamma_{\tau,\mathrm{Pf}}$	$\gamma_{\tau,\mathrm{Sl}}$						

2.2. ***Cell differentiation.*** During culmination there is a rapid increase in the number of cell types that are functionally different. We have not tried to describe every different cell type, but instead we have restricted our comments to the cell types that seem to play key roles in the extension of the stalk and the formation of the spore head. We did not have to take into account the basal disc and the upper and lower cup, or the transition of prespore cells into mature spore cells.

The process of cell differentiation as described in the Introduction is implemented in the following way: since PstA cells become stalk cells only when they enter the stalk tube, we assume an induction process for which cell–cell contact is necessary. This is implemented by searching PstA–stalk cell contacts at fixed time intervals ($\Delta t_{\mathrm{induction}}$) and by changing one PstA cell into a stalk cell. For each PstA cell the chance that the latter will occur is proportional to the amount of contact area. In the meantime PstO cells change into PstA cells, which is modelled in the same way. Note that we have used fixed time intervals to avoid instabilities in the transitions between the cell types. A very broad range of time intervals can be used, which affects only the height and thickness of the stalk.

While a PstA cell is differentiating into a stalk cell, it produces tube material; this is implemented by instantaneously increasing the target volume V of the stalk tube. And due to vacuolation the cell also increases its own volume. To model this process we slowly increase the target volume of stalk cells during the initial period following their appearance, i.e., during the first 10 000 time steps ($\pm$15 min when one time step represents 0.1 s), by 33%.

2.3. ***cAMP signalling.*** The cAMP plays a central role in our model. To describe the cAMP dynamics a discretized PDE is used with the same grid size as the CA. The cAMP can freely diffuse through all cells and through the slime sheath, but not through the tube, which is considered to be impermeable to cAMP, or into the air or substratum.

The cAMP dynamics can be described reasonably well in a quantitative way by simplified two-variable equations of the FitzHugh–Nagumo (FHN) type (Marée

et al., 1999a). Here we use FHN-type equations with piecewise linear 'Pushchino kinetics' (Panfilov and Pertsov, 1984):

$$\frac{\partial c}{\partial t} = D_c \Delta c - f(c) - r, \tag{4}$$

$$\frac{\partial r}{\partial t} = \varepsilon(c)(kc - r), \tag{5}$$

when cell type $\tau \in$ {Psp, PstO, PstA}, and

$$\frac{\partial c}{\partial t} = D_c \Delta c - d_c(c - c_0), \tag{6}$$

when cell type $\tau \in$ {St, Pf, Sl},
and with $f(c) = C_1 c$ when $c < c_1$; $f(c) = -C_2 c + a_\tau$ when $c_1 \leq c \leq c_2$; $f(c) = C_3(c-1)$ when $c > c_2$, and $\varepsilon(c) = \varepsilon_1$ when $c < c_1$; $\varepsilon(c) = \varepsilon_2$ when $c_1 \leq c \leq c_2$, and $\varepsilon(c) = \varepsilon_3$ when $c > c_2$. To make the function $f(c)$ continuous, $c_1 = a_\tau/(C_1 + C_2)$, and $c_2 = (a_\tau + C_3)/(C_2 + C_3)$. In these equations c represents the cAMP concentration, and r the refractoriness of the cells.

There seems to be evidence that PstA cells periodically produce the cAMP signal and PstO cells relay the signal (Kitami, 1984). This can be implemented in the model by giving the first cell type a negative value of a_τ, and the second cell type a positive value of a_τ (see Marée *et al*., 1999a). The prespore cells also relay the cAMP signal (see Discussion).

The response to the cAMP signal is a chemotactic movement towards the cAMP. We incorporate the chemotactic response by using the local cAMP spatial gradient: $\Delta H' = \Delta H - \mu(c_{\text{automaton}} - c_{\text{neighbour}})$, where $\Delta H'$ is the new change in energy. This makes it more likely that an amoeba will move towards a location with a higher cAMP concentration and less likely that it will move towards one with a lower cAMP concentration. Chemotaxis is only taken into account when cAMP is above a threshold $c_{\text{th}} = 0.05$ and refractoriness below a threshold $r_{\text{th}} = 0.2$. The stalk cells and pathfinder cells do not produce or relay the signal (Sternfeld, 1992) and they are not chemotactic (Williams *et al*., 1989), which means that they are not involved in the signalling or in the response. Remember that rapidly after differentiating the stalk cells die, and hence for these cells this is the only reasonable assumption.

2.4. ***Initial condition.*** The initial condition for our model is based on the following observations. When the slug halts its forward movement, the tip lifts up and the rear part crawls in underneath, and a more or less hemispherical shape is formed (Higuchi and Yamada, 1984). This is the moment that we have taken as our starting point. At this stage, the uppermost part consists of PstA cells, lower down are PstO cells, and at the bottom are the Psp cells (Williams *et al*., 1989). The initial core of pathfinder cells developed earlier, during the slug stage (Jermyn and Williams,

1991). We start our simulations when the stalk cell differentiation has just begun, presumably initially induced by the pathfinder cells. The stalk tube, however, has not yet formed. The stalk primordium is slightly submerged. If stalk formation were to start completely at the top, one would expect an invagination, but this is not observed. Hence it seems that cells somewhat deeper down in the culminant are involved in the prestalk–stalk transition (Watts and Treffry, 1976). Because the tube material is produced locally, the stalk cells are initially surrounded by this material.

The open space between the cells is filled with slime, a 'worst case scenario' to describe the fact that the slime material seems to be produced by all cells (Wilkins and Williams, 1995). This part of the initial condition is obviously very unrealistic. However, within a few time steps the slime spreads out over the cell mass and the slime sheath is formed. Clearly, this process of 'squeezing out' the slime and of slime sheath formation normally happens much earlier during development.

3. RESULTS

We were able to reproduce the culmination of *Dictyostelium discoideum*. Figure 1 shows a number of snapshots of the process. MPEG movies of the simulations are available on-line: `http://www-binf.bio.uu.nl/stan/bmb`.

We have scaled the time step and space step so as to simulate realistic values for the cAMP dynamics. To attain the (for the slug stage) characteristic periodicity of 2–3 min (Siegert and Weijer, 1992), one time step must correspond to 0.1 s. To obtain a signal propagation velocity around 200 μm/min (Siegert and Weijer, 1989), one grid point must correspond to 5 μm. This scaling produces the correct timescale for culmination and a fruiting body of the correct size: a fruiting body about 6 mm high is formed, in about 4 h.

Within a very short time-span, i.e., within 2 min, the tube material forms a tube round the stalk cells. The stalk tip, however, does not become surrounded by stalk tube; instead it is occupied by the pathfinder cells. The tube mouth is formed at the top of the stalk. Periodically cAMP waves, originating in the PstA region, move downwards through the cell mass. These waves combined with the chemotactic response towards the cAMP lead to upward cell motion. At the same time the stalk tip quickly moves downwards, apparently 'guided' by the pathfinder cells: the stalk elongation is directly perpendicular to the substratum, and the pathfinder cells continue to occupy the tip region. Within 20 min after passing through the prestalk/prespore interface the stalk arrives at the base. When the stalk reaches the substratum, the pathfinder cells anchor it and motion in the tip region halts. The culminant elongates upwards by continuous production of stalk cells combined with an upward motion of the spore mass. When the prestalk cell reservoir is empty, a spore head forms at the top of the stalk.

There are a number of processes which need to be looked at more closely: the formation of the tube, the fast downward elongation of the stalk, the fact that this

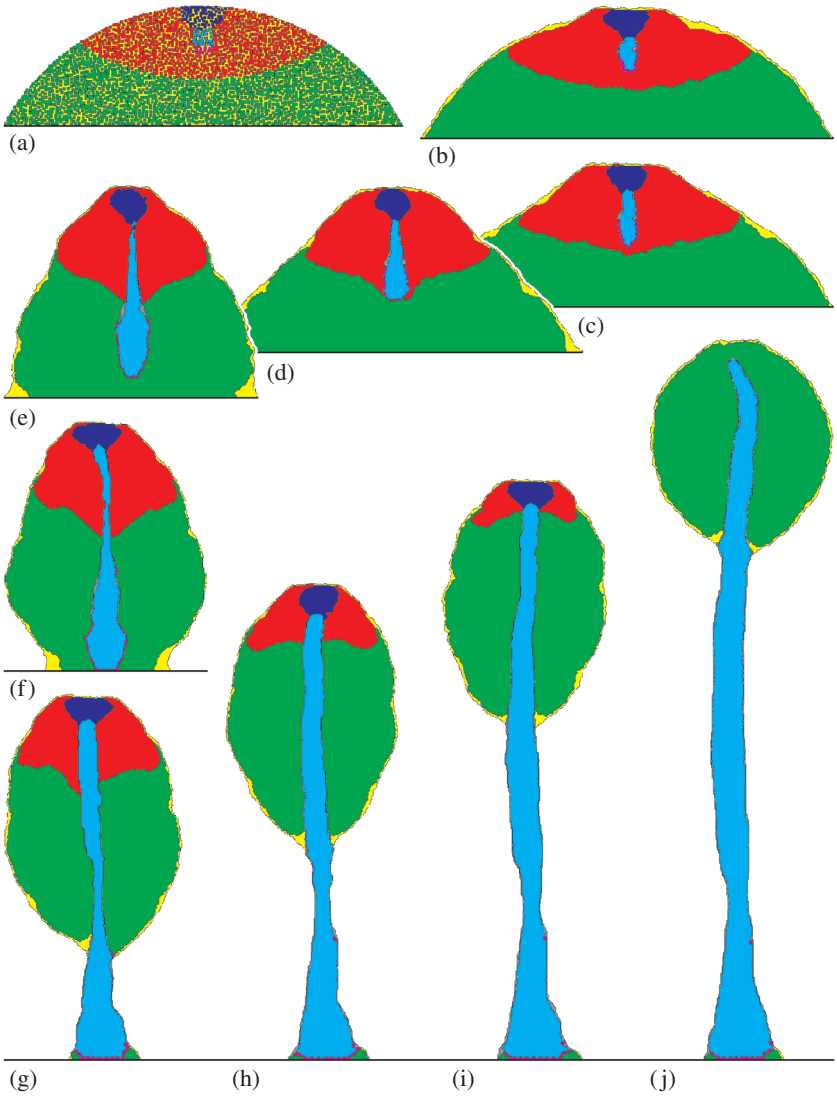

Figure 1. Time sequence of a simulation of the process of culmination. (a) Initial condition; (b) 2 min (1200 time steps); (c) 5 min (3000 time steps); (d) 10 min (6000 time steps); (e) 20 min (12 000 time steps); (f) 30 min (18 000 time steps); (g) 1 h (36 000 time steps); (h) 1 h 30 min (54 000 time steps); (i) 2 h (72 000 time steps); and (j) 4 h (144 000 time steps). There are 3089 cells. One time step (solution of the PDEs) corresponds to about 0.1 s, and one grid point to 5 μm. Cell types are $\tau \in$ {Psp (green), PstO (red), PstA (blue), St (cyan), Pf (magenta), Sl (yellow), Tu (grey)}. $T = 6$, $\lambda = 1$, $\mu = 200$, $H_{\text{diss}} = 0.8$, $H_{\text{tubediss}} = 30$, and $\Delta t_{\text{induction}} = 85$ (8.5 s). The other parameters are given in Table 1. The parameters used to describe the cAMP dynamics are $a_{\text{PstA}} = -0.1$, $a_{\text{PstO}} = a_{\text{Psp}} = 0.1$, $D_c = 1$, $C_1 = 20$, $C_2 = 3$, $C_3 = 15$, $\varepsilon_1 = 0.5$, $\varepsilon_2 = 0.0589$, $\varepsilon_3 = 0.5$, $k = 3.5$, $d_c = 0.05$, and $c_0 = -0.3$. The PDEs are solved by the explicit Euler method (with time step equal to 0.01 and space step equal to 0.37).

elongation is perpendicular to the substratum, the anchoring of the stalk when it reaches the base, and the final configuration.

3.1. ***Tube formation.*** The stalk tube is formed very quickly. Due to strong cell adhesion between the stalk cells and weak adhesion between stalk and PstO cells, the tube material is 'squeezed' outwards, where it accumulates at the boundary between the two cell types. The tube mouth remains open, i.e., the matrix does not extend over the top, due to the continuous formation of new stalk cells and the more moderate adhesion strength between stalk and PstA cells. It does not extend along the stalk tip either, because the pathfinder cells adhere strongly to both stalk cells and PstO cells. In addition, the stiffness of the tube slows down its extension, both along the stalk tip and the tube mouth.

3.2. ***Stalk elongation.*** The tip of the stalk elongates faster downwards than prestalk and prespore cells move upwards, although neither pathfinder cells nor stalk cells show a chemotactic response. Instead the pathfinder cells are pushed downwards by pressure waves that accompany the cAMP waves. Figure 2 'zooms in' on the process of downward motion. The figure shows the cAMP waves, the accompanying pressure waves, and the response of the pathfinder cells. Although chemotactic motion occurs only at the wavefront, directed motion is not confined to this region. Because cells push and pull each other, directed motion is observed over a very large area and takes place more or less all the time (Marée *et al.*, 1999a). A cAMP wave is always preceded by a period of low pressure, because cells are already pulled away, and is followed by a period of high pressure, because chemotactically active cells push the cell mass. The low pressure pulls the pathfinder cells outwards and the high pressure pushes them inwards again. Because the cAMP wave moves downwards, the pattern of pulling and pushing the pathfinder cells also moves downwards. This means that the pressure waves create a peristaltic motion of the stalk tip, which is comparable to the motion of the intestine. The peristaltic motion efficiently squeezes both pathfinder and stalk cells downwards. A little further up the pathfinder cells that move downwards are replaced by tube material. At the same time, but at the other end of the stalk, newly recruited stalk cells move into the tube. These cells are transported through the tube by the combination of pushing at the tube mouth, due to the surface tension between PstA and stalk cells, and pulling in the lower region, due to the peristaltic motion.

3.3. ***The role of cAMP and pathfinder cells in stalk elongation.*** The pressure waves are created by the chemotaxis towards cAMP. As a consequence, without periodic cAMP waves or chemotactic motion there will be no peristaltic motion and no displacement of the stalk. Figure 3 shows a simulation without cAMP dynamics. In this simulation, the culminant does not move upwards, and the stalk does not move downwards at all. Instead the cells just form one big cluster.

The pathfinder cells are also essential for stalk elongation. Figure 4(b) shows a simulation in which the pathfinder cells were omitted from the model. Now the

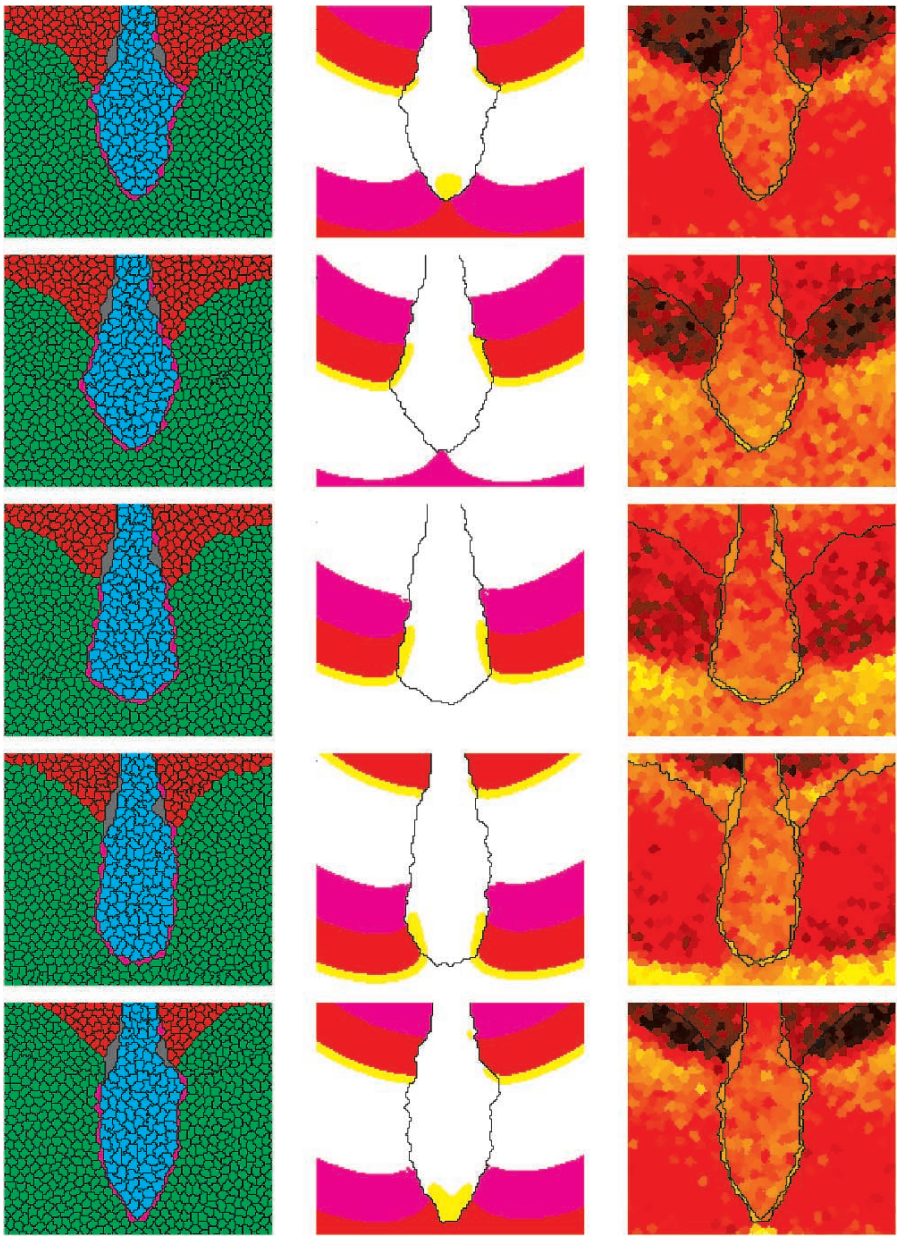

(a) Individual cells (b) cAMP waves (c) Pressure differences

Figure 2. Detailed view of the stalk elongation during the simulation of Fig. 1. (a) All individual cells. Colour-coding is the same as in Fig. 1; (b) propagation of the cAMP waves. Yellow shows the area where $c > c_{\text{th}}$ and $r < r_{\text{th}}$ (the wavefront); red the area where $c > c_{\text{th}}$ and $r > r_{\text{th}}$ (the waveback); and magenta represents the area where $c < c_{\text{th}}$ and $r > r_{\text{th}}$ (the refractory period). Cells only show chemotaxis in the yellow area; (c) pressure differences, indicated by the mean cell volume of individual cells, averaged from five samples at intervals of 2 s. Volumes are indicated by a colour gradient from dark red (small volume) to bright yellow (large volume). Top frame at 14 min 40 s (8800 time steps). Successive frames at intervals of 40 s (400 time steps).

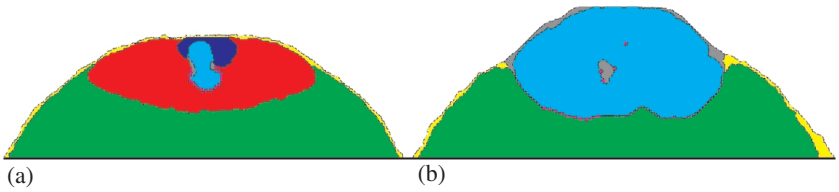

Figure 3. cAMP dynamics needed for stalk elongation. Without cAMP signalling the stalk does not elongate downwards, but instead all stalk cells lump together in the upper part. Two snapshots are shown. (a) 8 min 20 s (5000 time steps); and (b) 3 h (108 000 time steps). The simulation is done without cAMP; all other parameters are as described in the legend to Fig. 1.

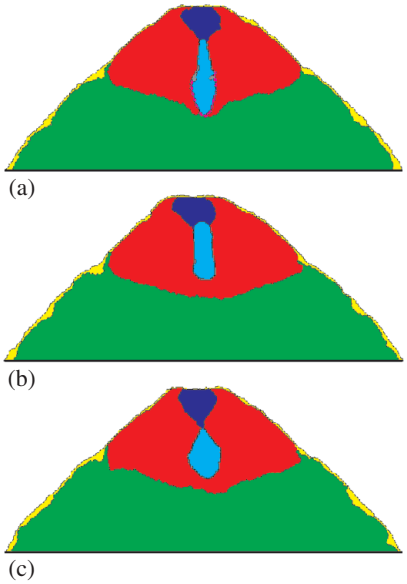

Figure 4. Pathfinder cells needed for stalk elongation. Snapshots are shown of a simulation with and two simulations without pathfinder cells. (a) Snapshot taken from the simulation of Fig. 1; (b) without pathfinder cells, the stalk does not extend downwards, due to the stiffness of the stalk tube; (c) when the stalk tube is flexible (H_{tubediss} equals H_{diss}), the upper side of the stalk becomes detached, and the stalk tip flattens. All snapshots are taken at the same moment, i.e., after 8 min 20 s (5000 time steps). All parameters (except H_{tubediss} in C) are as described in the legend to Fig. 1.

stalk tip also becomes surrounded by the stalk tube. A kind of bag is formed due to the stiffness of the tube. The structure is filled with an increasing number of stalk cells, but is unable to extend downwards or to keep its elongated shape. This is simply because the stiffness of the tube does not allow for any peristaltic motion. Figure 4(a) shows the culminant from the simulation of Fig. 1 at the same point of time. The stalk here does indeed extend much further.

But even if the tube were as flexible as all other entities, no normal stalk elongation would occur. Figure 4(c) shows that when we simulate a flexible tube, the

stalk rapidly loses its connection to the PstA region. This is due to the fact that in this case the stalk can be squeezed downwards everywhere along the tube, with the efficiency that was previously found only in the region around the stalk tip. Moreover, Fig. 4(c) shows that under these circumstances the stalk completely loses its elongated form. Instead, the shape very quickly becomes more or less round. This is due to the resistance created by all the cells that move upwards, which make it look like a falling drop of water. In contrast, in Fig. 4(a) such an effect cannot be observed. This is because with a stiff tube only the tip is easily pulled downwards; the rest of the stalk is much more resistant. Hence the stalk tip is pulled into a spiky shape. Such a shape efficiently reduces the resistance created by the upward moving cells and, in the long run, makes the whole stalk nicely elongated. The flat base of the 'stalk' without a stiff tube in Fig. 4(c) does indeed strongly reduce the downward elongation. In conclusion, both flexible pathfinder cells and a stiff tube are needed to make the fast descent of the stalk tip possible.

3.4. ***Correction of orientation.*** Pathfinder cells are necessary not only for the downward motion of the stalk and its elongated shape, they also ensure that the elongation is precisely in the opposite direction to the upward moving cells. This is really not trivial, since an elongated structure that moves against the flow always has a very strong tendency to bend sideways.

Figure 5 shows a simulation in which the stalk is initially bent 90 degrees. However, very rapidly the tip turns downwards again. Figure 6(b) shows the final configuration of this simulation, which does not differ much from the fruiting bodies of other simulations. The mechanism can be described as follows. Normally both sides of the stalk tip are pushed or pulled at the same time. Stalk cells are transported downwards, from the region where the stalk tip is pushed to the region where it is pulled. A different situation arises when the tip no longer points downwards, for example due to the combined effect of random fluctuations and the force exerted by the cells moving upwards. Now the cAMP waves no longer move perpendicular to the stalk, but arrive at one side sooner than at the other. Consequently, at the moment one side is pushed, the other side is still being pulled. This efficiently transports cells inwards, instead of downwards, and the original orientation is restored. Note that along the side which is pushed there is also a region which is pulled, and along the other side there is also a region that is pushed. These regions, however, are not located opposite to each other, and hence this does not lead to efficient cell transport.

Peristalsis also explains the position of the pathfinder cells. When more than half of the pathfinder cells happen to be positioned along one side of the stalk, the imbalance is quickly rectified. This is because downward motion on the more crowded side is more efficient and pushes the cells back to the other side. Hence the pathfinder cells always remain positioned along the tip of the stalk, yet another property which was not explicitly incorporated in the model.

In conclusion, the stalk tip always extends perpendicular to the cAMP waves,

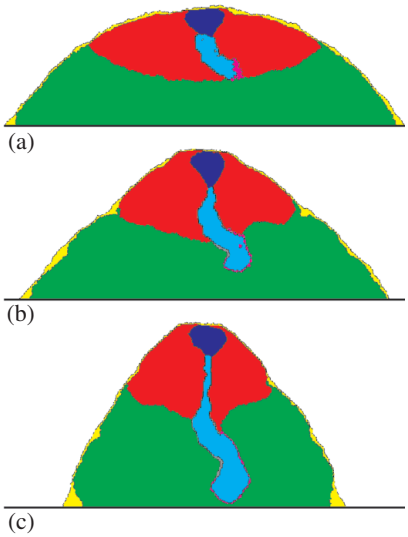

Figure 5. Correction of the direction of stalk elongation. In the initial configuration the stalk tip is bent 90 degrees. (a) 50 s (500 time steps); (b) 8 min 20 s (5000 time steps); and (c) 16 min 40 s (10 000 time steps). The final fruiting body is shown in Fig. 6(b). All parameters are as described in the legend to Fig. 1.

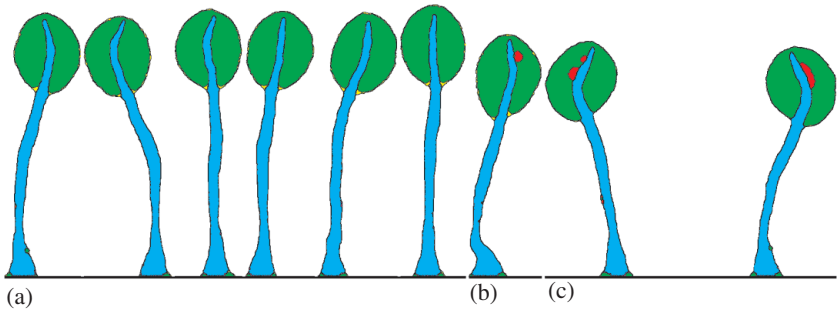

Figure 6. Variations in the final fruiting bodies that were formed by (a) six simulations with different random seeds; (b) the simulation of Fig. 5, in which the stalk tip was initially bent 90 degrees; and (c) the simulation of Fig. 7, in which two fruiting bodies orient away from each other. The precise final configuration varies, but they all have the same general appearance. All parameters are as described in the legend to Fig. 1.

and any deviations are corrected. Since the tip of the culminant is the source of the cAMP waves, and is on top of the culminant, the stalk becomes positioned more or less perpendicular to the substratum.

3.5. ***Anchoring.*** Due to the mechanism described above the downward motion stops automatically: when the stalk tip reaches the base, it is no longer completely surrounded by cAMP waves, and therefore it does not move further downwards. The pathfinder cells which have not yet reached the base still have a tendency to move downwards but not sideways. Therefore, all pathfinder cells finally end up

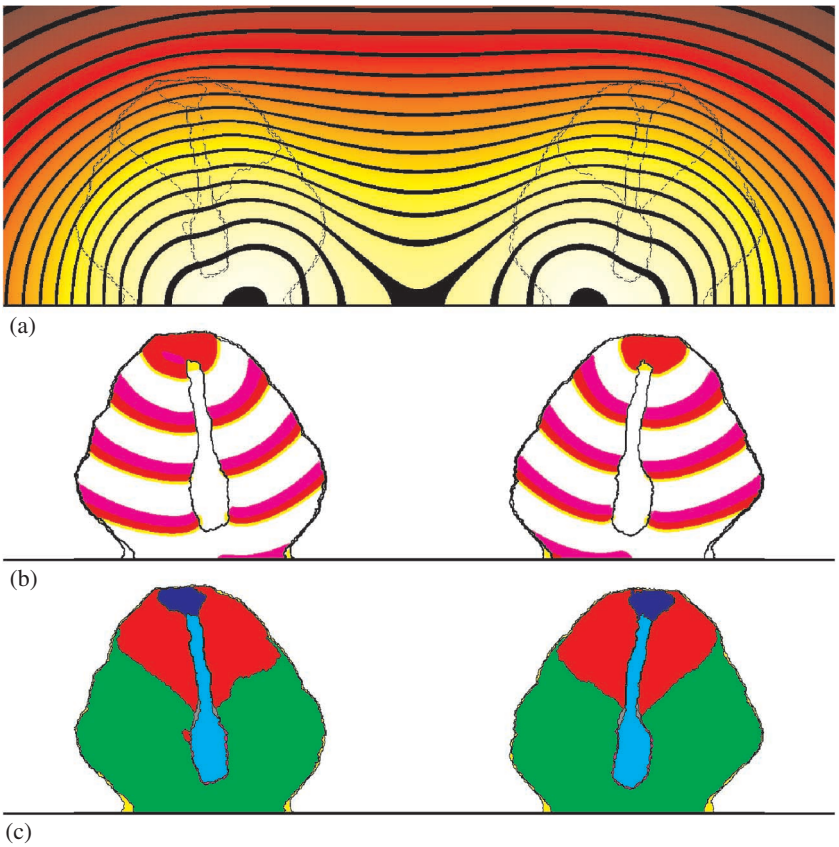

Figure 7. Two culminants orienting away from each other due to NH_3 production. (a) Shows the NH_3 distribution; (b) shows the cAMP waves; and (c) shows the culminants with slanted stalks. Time is 20 min (12 000 time steps). Colour-codings in (b) and (c) are the same as in Fig 2. The NH_3 distribution is indicated by a colour gradient from dark red (low concentration) to bright yellow (high concentration). The black lines are curves of iso-concentration. All prestalk and prespore cells produce 1×10^{-3} NH_3/s. We have used a diffusion constant of 15. The inhibiting effect of the NH_3 on the cAMP dynamics is implemented in the following way: $a(\tau, n) = a_\tau + \frac{b_\tau n^s}{1+(n/p)^s}$, with $a_{\mathrm{PstA}} = -0.20$, $a_{\mathrm{PstO}} = a_{\mathrm{Psp}} = -0.025$, $b_{\mathrm{PstA}} = 0.0375$, $b_{\mathrm{PstO}} = b_{\mathrm{Psp}} = 0.075$, $p = 2$, and $s = 3$. The NH_3 dynamics are solved by the implicit ADI method. All other parameters are as described in the legend to Fig. 1.

on the substratum, and the stalk tube surrounds the whole stalk. Obviously, in our model the pathfinder cells adhere quite strongly to the substratum, but this is not very important for the general behaviour.

3.6. ***Final configuration.*** New stalk is continuously added at the tube mouth until all prestalk cells are transformed into stalk cells. When the PstA cell type is exhausted, the cAMP waves also cease, because it is only the PstA cells that periodically produce the cAMP signal. Therefore, the moment the stalk formation

is complete, the upward motion halts. After the chemotactic motion has stopped, the prespore cell mass becomes rounded, due to surface tension properties. The tube, however, is too stiff to change its general shape. Hence, in the model, a globule of spores on a slender stalk is a stable configuration.

The upward extension of the stalk is not specifically guided, and because of that some deviations in the direction of outgrowth can be observed. Figure 6(a) shows that due to random fluctuations during the culmination, the precise final configuration does indeed vary, but the fruiting body retains its general appearance. These two features are also observed *in vivo* (Bonner and Dodd, 1962).

Since in our model the process of culmination is so closely related to the cAMP dynamics, it it clear that any process that changes the cAMP waves will also change the final configuration of the culminant. In Marée *et al*. (1999b) we showed that because NH_3 inhibits the cAMP-induced cAMP release (Williams *et al*., 1984), NH_3 could play a key role in a number of tactic behaviours, especially phototaxis. Here we show that the default NH_3 production by the cells and its effect on the cAMP dynamics, combined with the sensitivity of the culmination process for such modulations, can account for the well-known phenomenon of culminants orienting away from each other (Feit and Sollitto, 1987). Figure 7 shows a simulation in which the cells produce a small amount of NH_3, which diffuses away into the air. The effect of NH_3 is implemented by increasing the threshold for the cAMP response, as described in Marée *et al*. (1999b). NH_3 accumulates between the culminants, which decreases the excitability along the two sides that face each other. Because cAMP waves move more slowly at lower excitability, the waves become slanted (Marée *et al*., 1999a); and since the stalks extend perpendicular to the cAMP waves, they move towards each other instead of straight downwards. Therefore we end up with fruiting bodies that are oriented away from each other [see Fig. 6(c)]. Note that in this simulation the culminants are positioned closer to each other than is normally observed in nature. The distance that we have used, however, has been dictated by computational limitations.

3.7. ***Cell adhesion.*** Adhesion plays an important role in the model behaviour. To reproduce all the dynamics of the culmination, the surface tensions γ, as defined in equations (2) and (3), were adjusted in the following ways.

The γ between the the PstA, PstO and Psp cells are such that they adhere to each other, but form fairly homogeneous groups. The γ between PstA and Psp is slightly higher so that all prestalk cells will remain together when the end of the culmination approaches.

By using 'normal' γ between the slime and the various cell types *and* between the slime and the air, whereas the γ between the various cell types and the air in fact are very high, a slime sheath is formed that completely surrounds the culminant. Similarly, because the γ between the tube material and the PstO and Psp cells are 'normal', whereas the γ between the stalk cells and these cell types are very high, the stalk tube is formed. The γ between the stalk tube and the air is 'normal', and

the γ between the stalk tube and the slime sheath is low (but not zero), so that the fruiting body will be surrounded by slime sheath and stalk tube, but both matrices will not intermingle.

Because of the differences in the γ between the three main cell types and the slime sheath, the Psp cells have a tendency to engulf the PstO cells, which, in their turn, have a tendency to engulf the PstA cells (Takeuchi *et al*., 1988). This helps as a compensation for the decreased upward motion close to the slime sheath. Upward motion is slower there due to some inward and outward motion, which smooths the pressure waves. These differences in γ also ensure that the spore head is eventually completely on top of the stalk.

The γ between the pathfinder cells and the PstO and Psp cells are very low, so that they can move smoothly through the cell mass. Also the γ between the pathfinder cells and the stalk cells and stalk tube are very low, so that the pathfinder cells can pull them downwards easily. The γ between the pathfinder cells and the Psp cells is lower than the γ between the pathfinder cells and the PstO cells, so that the pathfinder cells can move smoothly through the PstO–Psp interface. The same is done for the stalk tube.

The tension between the stalk cells and PstA cells is quite high, to ensure that stalk cells are pushed into the stalk tube, as a result of the surface tension. Because the γ between the pathfinder cells and the substratum is low, but between the stalk cells and the substratum is high, the pathfinder cells form the base of the stalk, and hence more or less determine the width of the inner part of the 'basal disc'.

4. DISCUSSION

The 'reverse fountain' is the wonderful culmination of *Dictyostelium discoideum* morphogenesis. So far, however, no satisfactory explanation for this phenomenon has been given in the literature. Often it has simply been considered as a fact. For example, Jermyn and Williams (1991) state that the reverse fountain directs the PstA cells into the entrance of the stalk tube and that the tip extends downwards by the accretion of PstA cells at the entrance. In our model, a reverse fountain has not been defined; instead, it emerges from the local transition rules.

We have demonstrated the occurrence of the reverse fountain on the basis of (i) periodic waves of chemotaxis; (ii) flexible pathfinder cells; and (iii) a stiff tube.

4.1. ***Stalk formation.*** We have shown that periodic chemotactic motion towards cAMP waves creates periodic pressure modulations, which move downwards together with the cAMP waves. The flexible stalk tip, which is not chemotactic, is squeezed downwards by the peristaltic motion that is created by these 'pressure waves'. Because the pressure waves move in the same direction as the stalk, this process can occur much faster than normal chemotactic cell motion. The stalk tip pulls the stalk tube with it, although it resists movement due to its stiffness. New

stalk cells are transported through the tube by the combined pushing at the apex and pulling at the base. Because the process of stalk elongation is so closely linked to the cAMP dynamics, the direction of the extending stalk can be maintained, and its displacement automatically halts when it reaches the base.

Hitherto, some authors have assumed that stalk elongation is due to the the fact that the stalk is pushed downwards through the culminant by the accretion of prestalk cells at the tube mouth (Jermyn and Williams, 1991; Thomason *et al*., 1999). However, with our model we can show that the addition of new stalk cells at the apex cannot be responsible for the fast and straight downward motion of the stalk, due to a number of mechanical problems. First of all, pushing the stalk downwards becomes increasingly more difficult during stalk formation, because the force is exerted only on a very small surface, whereas the frictional force, which is exerted over the whole surface of the stalk, increases linearly with stalk length. Secondly, because the whole cell mass moves upwards, and the force is exerted only at the apex, the stalk will have a strong tendency to move sideways. And thirdly, if the force exerted at the apex is strong enough to let the stalk reach the base (which in our model is only feasible by simulating extremely small culminants), then the tip will simply continue to extend, even after it reaches the substratum. But because the stalk cannot move further downwards, it flips to one side, and extends laterally. Strong adhesion to the substratum does not prevent this. In contrast, the above complications are not encountered with the mechanism that we propose.

An alternative mechanism might be that the stalk is pushed downwards by prestalk cells on the outside of the tube, which, during the upward motion, push off against the stalk. A similar mechanism has been proposed for slug migration (Odell and Bonner, 1986). The model-formalism we use, however, ignores the fact that forces exerted to overcome friction and to accelerate lead to similar counterforces. Implicitly we assume that counterforces are simply passed on to neighbouring cells and extracellular matrix, and spread out without influencing the local motion. However, even if this assumption turns out to be incorrect and such forces are nevertheless able to influence stalk displacement, this alternative mechanism still cannot explain why the stalk should become elongated in the first place. Nor can the mechanism account for the extremely fast downward motion, or for the correction of orientation.

4.2. ***cAMP signalling.*** In our model cAMP signalling is a prerequisite for normal stalk development and fruiting body formation (see Fig. 3). However, serious doubts have been expressed in the literature about whether chemotaxis continues to play a role during culmination, especially with respect to the prespore cells (Sternfeld, 1998). The alternative idea is that the growing stalk provides the force that carries the prespore cells aloft (Thomason *et al*., 1999). However, Watts and Treffry (1976) found that mature spores are not visible until the fruiting body reaches its maximum height, and Kitami (1984) showed that during culmination both prestalk and prespore cells are still able to exhibit a chemotactic response

to cAMP. Besides, Chen *et al*. (1995, 1998) showed that normal culmination is impaired when the rate of chemotactic motion is reduced. They showed that a chemotactic response by the prestalk cells only, or by the prespore cells only, is not sufficient for normal culmination. They conclude that prespore cells play a more active role than previously assumed. Another clue is that prespore cells, during their ascent of the stalk, are sometimes observed to move in a spiral pattern, a behaviour that cannot be passive (Kessin, 2001).

Because the stalk tip is oriented by cAMP waves, the same processes that alter the cAMP waves should also alter the stalk orientation. The fact that culminants are able to influence each other (Bonner and Dodd, 1962), such as orienting away from each other (Feit and Sollitto, 1987), can therefore simply be due to their own NH_3 production and the effect it has on the cAMP dynamics (see Fig. 7). Moreover, because temperature and light conditions influence the NH_3 production, thermotactic and phototactic orientations can also be expected during the culmination stage (see Marée *et al*., 1999a,b).

4.3. ***Model considerations.*** In our model a central role is reserved for cell–cell and cell–substratum adhesion. There is a vast amount of experimental evidence that supports differential adhesion between cell types and between the cells and the substratum in *Dictyostelium*, and stresses the importance of adhesion during development. For reviews on the role of adhesion in *Dictyostelium*, see Fontana (1995) and Bozzaro and Ponte (1995). Tuning our model has produced expected parameters for adhesion strengths between cell types. Hence we predict that the same relations between adhesion strengths will be found in experiments. However, one has to bear in mind that in the model the J_{τ_1,τ_2} values represent effective cell adhesions, in which several processes are lumped together. Hence it may prove difficult to relate them directly to experimental observations.

We have restricted the set of entities used in our model to the ones that are needed to obtain a good description of the reverse fountain. The pathfinder cells are essential in our model. If they are omitted, then the stiff tube material will surround the stalk tip and no peristaltic motion will be possible; a stiff bag will be formed instead of an elongating stalk. This problem cannot be solved by simply using a more flexible stalk tube (or by implementing pathfinder cells only and no tube, which produces more or less the same results). First of all, the stiff stalk tube has to support the fruiting body: without it the culminant will collapse. Secondly, the stiffness is needed to prevent downward motion of the complete stalk, as well as to give the stalk tip its typical wedge-like shape (as described by Higuchi and Yamada, 1984), which allows it to penetrate easily through the upward moving cell mass.

In our model we assumed a clear distinction between the PstA and PstO cells. Jermyn and Williams (1991) however showed that there is no entirely distinct class of PstO cells, but there is a discontinuous gradient in gene expression, with cells in the top one-tenth expressing the PstA marker most strongly. Because the cell differentiation seems to be a gradual process, the excitability and adhesion strengths can

also be expected to change more gradually. For reasons of convenience we have modelled the cell-type transition as an instantaneous process. However, we expect that the results will still hold even if the induction process is neither instantaneous nor local, as long as the properties connected with adhesion and excitability change together. This is important because the cAMP dynamics may not be disturbed too much during the time it takes for the newly formed PstA cells to sort out to the tip, which in the model is due to the interplay between the chemotaxis and differential adhesion (Marée *et al*., 1999a). Hence, if there is a co-regulation between adhesion strength and excitability, this would be strong support for the mechanism we propose.

The volume increase of the stalk cells occurring due to vacuolation is not very important for the model behaviour. In contrast, Higuchi and Yamada (1984) postulated that this process must be responsible for the downward elongation. We find, however, that the volume increase has a relatively small effect. The supply of stalk cells at the stalk tip is indeed greater when volume increase is larger, which helps to increase the downward velocity. However, in the model the vacuolation can be removed completely without causing a qualitative change in behaviour.

The stalk tube seems to become even more solid when exposed to the air (Higuchi and Yamada, 1984). But even before the stalk comes in contact with the air the tube is already stiff enough for it to be located by its resistance to the passage of a fine glass needle through the tissue (Sternfeld, 1992). No gradual change in stiffness is needed in the model, and therefore we have not implemented this feature.

Neither have we implemented any processes relating to the upper and lower cup, because they are not directly needed for either elevating the cell mass or preserving the final shape of the fruiting body. And we observe in the model that even if there is no specific cell type connected to the basal disc, something comparable is nevertheless created, with a core formed by the stalk tip, and an outer ring formed by 'rearguard' cells that are left behind.

However, some of the above processes that are not essential for the culmination as described above could play all kinds of other roles during the development. For example, it could very well be that the turgor pressure of the highly vacuolated cells contributes to the maintenance of the final stalk structure (Watts and Treffry, 1976).

In our simulations we do not find the typically observed extended shape of the tip. We expect that this specific form of the tip is a three-dimensional (3D) property, caused by 3D scroll waves, and hence cannot be depicted in our 2D simulations. Such scroll waves have been found to organize the tip region during the slug stage (Siegert and Weijer, 1992). Scroll waves may also explain the early formation of the stalk primordium, because in the core of the scroll wave one finds a permanently low cAMP concentration (Siegert and Weijer, 1992), and during the slug stage low cAMP levels are needed to induce differentiation into pathfinder cells (Berks and Kay, 1990).

Finally, there is also another consequence of performing 2D instead of 3D simulations. Because the stalk is much narrower than the prestalk area that forms it,

the stalk can become very long. However, due to scaling properties, this effect is quadratically larger in 3D than in 2D. Hence, to produce a fruiting body of normal height in 2D, the culminant must be initially four times as broad.

4.4. ***Side-effects.*** The mechanisms described here not only generate the dynamics that are directly connected with the unfolding of the reverse fountain, but, as a side-effect, they can also give rise to a number of seemingly unrelated features. Nevertheless, many of these features are observed in experiments. Thus, in our model, no extra assumptions are needed to explain such features.

Harwood *et al*. (1992) showed that when the differentiation of PstA cells into stalk cells is blocked, and hence no stalk is formed, the culminant continues to extend. This process does not stop, and eventually the culminant becomes an erratic hair-like structure, which collapses onto the substratum. In our model, we can perceive the same kind of behaviour because the upward motion is due to chemotaxis—not to stalk extension, as previously assumed (Thomason *et al*., 1999)—and because the upward motion does not stop, due to the fact that the PstA cell pool is never emptied and hence cAMP waves keep on being produced.

Kitami (1985) showed that when a culminant is exposed to a centrifugal force of 40–50 **g**, hardly any cell mass can culminate (it remains shaped like a mound). When a cell mass did not culminate, it did not form a normal stalk. This one-to-one relation between upward motion of the cells and downward motion of the stalk (see Fig. 3) logically follows from the mechanism we propose.

In our model, the mechanism that corrects the direction of elongation does not work if we commence with a small isolated cluster of cells: the cells form a rounded mass, show no efficient peristaltic motion and are pushed sideways by the upward moving cells. This corresponds to the description that Sternfeld (1992) gives of the small clusters of early stalk cells that are formed during the late slug stage: sometimes 25–50 cells separate, expand a little and attain a surface position before they finally reach the rear of the slug.

We also observe a constriction at the base of the prespore zone before the stalk reaches the substratum. In our model, this is simply due to the combination of adhesion and upward motion. Neither a spiralling motion nor a contractile event at the surface of the cell mass is required to produce this constriction (Chen *et al*., 1998, suggested that these factors might be needed to explain the constriction).

After the stalk tip reaches the base, the stalk becomes slightly thickened, as observed by Higuchi and Yamada (1984). If we look at the final configuration, with the globule of spores on a slender stalk, we see that the spore head is still enclosed by the slime sheath, both in our simulations and *in vivo*. This may indeed be important for holding together the mass of spores (Watts and Treffry, 1976), but no ‘new’ features are needed. The stalk is surrounded by the stalk tube, but the tube material neither envelops the spore head nor the cells that are left on the substratum, again as *in vivo* (Watts and Treffry, 1976).

And finally, Sternfeld (1992) found that the outer ring of the basal disc consists only of a single layer of rearguard cells: the major portion of the basal disc is formed by the downward moving stalk. In our simulations, a basal disc-like shape is formed, with an outer ring of cells that fail to move upwards with the mass of prespore cells. To obtain this behaviour we do not have to define basal-disc cells or rearguard cells.

4.5. ***Conclusions.*** In this study, we have largely ignored the genetics and detailed regulatory mechanisms of *Dictyostelium discoideum*. As a result, our model allows us to pinpoint those elements that are essential for the successful formation of a fruiting body: we have shown that the whole process can unfold in a minimal model with fixed parameters. Nevertheless, it is known that many genes are up- and down-regulated during culmination, and research in the near future is likely to reveal much more about the high number of genes involved. If one wants to relate gene knowledge to this model, it is important to take the following points into consideration. First of all, many of these genes are connected to processes not directly related to the cell movements, such as, for example, the maturation of spore cells. Nevertheless, a large set of genes is needed for each process that we have described in the model. And these processes must be fine-tuned, which again requires a number of genes. Moreover, all processes have to be operational under many different circumstances. Therefore, by evaluating the role of those genes that are involved in cell movement in the light of our model, one should be able to generate interesting insights into evolutionary refinements of the culmination process, as well as into genetic robustness and redundancy. Finally, because the model is completely defined at the (sub)cellular level, whereas the mechanisms at work are on larger scales, one can begin to understand how gene expression can govern macro-level phenomena. For example, using this model it should be feasible to interpret the aberrant phenotypes that are created by restriction enzyme-mediated integration (REMI) (Smith, 2000).

We have used the hybrid CA/PDE model-formalism, because this formalism can describe the interaction between signalling, adhesion, pressure, pushing and pulling in a very elegant way. Our explanation for the dynamics during culmination is based on the interactions of these processes. These processes are the same as those which play the central role during the earlier stages of the development: here we have described the culmination, but previously we have used the model-formalism to explain how single amoebae aggregate into a mound, which eventually leads to the formation of the slug (Savill and Hogeweg, 1997). Later on we used the same formalism to unravel the mechanisms behind the thermotactic and phototactic properties that direct a slug to a suitable site for culmination (Marée *et al*., 1999a,b). Thus, we can now describe all the stages of the morphogenesis with one formalism. In summary, our model of the culmination of *Dictyostelium discoideum* culminates the modelling of its development.

ACKNOWLEDGEMENTS

We would like to thank Dr S M McNab for linguistic advice. AFMM was financially supported by the Priority Program Nonlinear Systems of the Netherlands Organization for Scientific Research.

REFERENCES

Amagai, A., S. Ishida and I. Takeuchi (1983). Cell differentiation in a temperature-sensitive stalkless mutant of *Dictyostelium discoideum*. *J. Embryol. Exp. Morphol.* **74**, 235–243.

Berks, M. and R. R. Kay (1990). Combinatorial control of cell differentiation by cAMP and DIF-1 during development of *Dictyostelium discoideum*. *Development* **110**, 977–984.

Blanton, R. L. (1997). Cellulose biogenesis in *Dictyostelium discoideum*, in *Dictyostelium: A Model System for Cell and Developmental Biology*, Y. Maeda, K. Inouye and I. Takeuchi (Eds), Tokyo: Universal Academy Press, pp. 379–391.

Bonner, J. T., A. D. Chiquoine and M. Q. Kolderie (1955). A histochemical study of differentiation in the cellular slime molds. *J. Exp. Zool.* **130**, 133–157.

Bonner, J. T. and M. R. Dodd (1962). Aggregation territories in the cellular slime molds. *Biol. Bull.* **122**, 13–24.

Bonner, J. T., H. B. Suthers and G. M. Odell (1986). Ammonia orients cell masses and speeds up aggregating cells of slime moulds. *Nature* **323**, 630–632.

Bozzaro, S. and E. Ponte (1995). Cell adhesion in the life cycle of *Dictyostelium*. *Experientia* **51**, 1175–1188.

Bretschneider, T., F. Siegert and C. J. Weijer (1995). Three-dimensional scroll waves of cAMP could direct cell movement and gene expression in *Dictyostelium* slugs. *Proc. Natl. Acad. Sci. U.S.A.* **92**, 4387–4391.

Bretschneider, T., B. Vasiev and C. J. Weijer (1999). A model for *Dictyostelium* slug movement. *J. Theor. Biol.* **199**, 125–136.

Chen, T.-L. L., P. A. Kowalczyk, G. Ho and R. L. Chisholm (1995). Targeted disruption of the *Dictyostelium* myosin essential light chain gene produces cells defective in cytokinesis and morphogenesis. *J. Cell Sci.* **108**, 3207–3218.

Chen, T.-L. L., W. A. Wolf and R. L. Chisholm (1998). Cell-type-specific rescue of myosin function during *Dictyostelium* development defines two distinct cell movements required for culmination. *Development* **125**, 3895–3903.

Clow, P. A., T.-L. L. Chen, R. L. Chisholm and J. G. McNally (2000). Three-dimensional in vivo analysis of *Dictyostelium* mounds reveals directional sorting of prestalk cells and defines a role for the myosin II regulatory light chain in prestalk cell sorting and tip protrusion. *Development* **127**, 2715–2728.

Dormann, D., B. Vasiev and C. J. Weijer (1998). Propagating waves control *Dictyostelium discoideum* morphogenesis. *Biophys. Chem.* **72**, 21–35.

Dormann, D., B. Vasiev and C. J. Weijer (2000). The control of chemotactic cell movement during *Dictyostelium* morphogenesis. *Phil. Trans. R. Soc. Lond. B. Biol. Sci.* **355**, 983–991.

Feit, I. N. and R. B. Sollitto (1987). Ammonia is the gas used for the spacing of fruiting bodies in the cellular slime mold, *Dictyostelium discoideum*. *Differentiation* **33**, 193–196.

Fontana, D. R. (1995). *Dictyostelium discoideum* cohesion and adhesion, in *Principles of Cell Adhesion*, P. D. Richardson and M. Steiner (Eds), Boca Raton: CRC Press, pp. 63–86.

Glazier, J. A. and F. Graner (1993). Simulation of the differential adhesion driven rearrangement of biological cells. *Phys. Rev. E* **47**, 2128–2154.

Grimson, M. J., C. H. Haigler and R. L. Blanton (1996). Cellulose microfibrils, cell motility, and plasma membrane protein organization change in parallel during culmination in *Dictyostelium discoideum*. *J. Cell Sci.* **109**, 3079–3087.

Harwood, A. J., N. A. Hopper, M.-N. Simon, D. M. Driscoll, M. Veron and J. G. Williams (1992). Culmination in *Dictyostelium* is regulated by the cAMP-dependent protein kinase. *Cell* **69**, 615–624.

Higuchi, G. and T. Yamada (1984). A cinematographical study of cellular slime molds. I. Stalk and disk formation in *Dictyostelium discoideum*. *Cytologia* **49**, 841–849.

Höfer, T., J. A. Sherratt and P. K. Maini (1995). *Dictyostelium discoideum*: cellular self-organization in an excitable biological medium. *Proc. R. Soc. Lond. Ser. B* **259**, 249–257.

Jermyn, K., D. Traynor and J. Williams (1996). The initiation of basal disc formation in *Dictyostelium discoideum* is an early event in culmination. *Development* **122**, 753–760.

Jermyn, K. A. and J. G. Williams (1991). An analysis of culmination in *Dictyostelium* using prestalk and stalk-specific cell autonomous markers. *Development* **111**, 779–787.

Jiang, Y., H. Levine and J. Glazier (1998). Possible cooperation of differential adhesion and chemotaxis in mound formation of *Dictyostelium*. *Biophys. J.* **75**, 2615–2625.

Kawasaki, Y., T. Kiryu, K. Usui and H. Mizutani (1990). Growth of the cellular slime mold, *Dictyostelium discoideum*, is gravity dependent. *Plant Physiol.* **93**, 1568–1572.

Keller, E. F. and L. A. Segel (1970). Initiation of slime mold aggregation viewed as an instability. *J. Theor. Biol.* **26**, 399–415.

Kessin, R. H. (2001). *Dictyostelium: Evolution, Cell Biology, and the Development of Multicellularity*, Developmental and Cell Biology Series **38**, Cambridge: Cambridge University Press.

Kitami, M. (1984). Chemotactic response of *Dictyostelium discoideum* cell to c-AMP at the culmination stage. *Cytologia* **49**, 257–264.

Kitami, M. (1985). Motive force of the culminating mass of cells in the developing fruiting body of *Dictyostelium discoideum*. *Cytologia* **50**, 109–115.

Levine, H. and W. Reynolds (1991). Streaming instability of aggregating slime mold amoebae. *Phys. Rev. Lett.* **66**, 2400–2403.

MacKay, S. A. (1978). Computer simulation of aggregation in *Dictyostelium discoideum*. *J. Cell Sci.* **33**, 1–16.

Marée, A. F. M. and P. Hogeweg (2001). How amoeboids self-organize into a fruiting body: multicellular coordination in *Dictyostelium discoideum*. *Proc. Natl. Acad. Sci. U.S.A.* **98**, 3879–3883.

Marée, A. F. M., A. V. Panfilov and P. Hogeweg (1999a). Migration and thermotaxis of *Dictyostelium discoideum* slugs, a model study. *J. Theor. Biol.* **199**, 297–309.

Marée, A. F. M., A. V. Panfilov and P. Hogeweg (1999b). Phototaxis during the slug stage of *Dictyostelium discoideum*: a model study. *Proc. R. Soc. Lond. Ser. B* **266**, 1351–1360.

Miura, K. and F. Siegert (2000). Light affects cAMP signaling and cell movement activity in *Dictyostelium discoideum*. *Proc. Natl. Acad. Sci. U.S.A.* **97**, 2111–2116.

Nanjundiah, V. (1973). Chemotaxis, signal relaying and aggregation morphology. *J. Theor. Biol.* **42**, 63–105.

Odell, G. M. and J. T. Bonner (1986). How the *Dictyostelium discoideum* grex crawls. *Phil. Trans. R. Soc. Lond. Ser. B* **312**, 487–525.

Palsson, E. and H. G. Othmer (2000). A model for individual and collective cell movement in *Dictyostelium discoideum*. *Proc. Natl. Acad. Sci. U.S.A.* **97**, 10448–10453.

Panfilov, A. V. and A. M. Pertsov (1984). Vortex ring in a three-dimensional active medium described by reaction-diffusion equations. *Dokl. Akad. Nauk SSSR* **274**, 1500–1503.

Parnas, H. and L. A. Segel (1977). Computer evidence concerning the chemotactic signal in *Dictyostelium discoideum*. *J. Cell Sci.* **25**, 191–204.

Rubinow, S. I., L. A. Segel and W. Ebel (1981). A mathematical framework for the study of morphogenetic development in the slime mold. *J. Theor. Biol.* **91**, 99–113.

Savill, N. J. and P. Hogeweg (1997). Modeling morphogenesis: from single cells to crawling slugs. *J. Theor. Biol.* **184**, 229–235.

Siegert, F. and C. Weijer (1989). Digital image processing of optical density wave propagation in *Dictyostelium discoideum* and analysis of the effects of caffeine and ammonia. *J. Cell Sci.* **93**, 325–335.

Siegert, F. and C. J. Weijer (1992). Three-dimensional scroll waves organize *Dictyostelium* slugs. *Proc. Natl. Acad. Sci. U.S.A.* **89**, 6433–6437.

Siegert, F. and C. J. Weijer (1995). Spiral and concentric waves organize multicellular *Dictyostelium* mounds. *Curr. Biol.* **5**, 937–943.

Smith, D. (2000). Completed and near-complete 80 REMI genes [online] <www-biology.ucsd.edu/others/dsmith/REMIgenes2000.html>.

Sternfeld, J. (1992). A study of PstB cells during *Dictyostelium* migration and culmination reveals a unidirectional cell type conversion process. *Roux's Arch. Dev. Biol.* **201**, 354–363.

Sternfeld, J. (1998). The anterior-like cells in *Dictyostelium* are required for the elevation of the spores during culmination. *Dev. Genes Evol.* **208**, 487–494.

Takeuchi, I., T. Kakutani and M. Tasaka (1988). Cell behavior during formation of prestalk/prespore pattern in submerged agglomerates of *Dictyostelium discoideum*. *Dev. Genet.* **9**, 607–614.

Thomason, P., D. Traynor and R. Kay (1999). Taking the plunge. Terminal differentiation in *Dictyostelium*. *Trends Genet.* **15**, 15–19.

Tyson, J. J. and J. D. Murray (1989). Cyclic AMP waves during aggregation of *Dictyostelium* amoebae. *Development* **106**, 421–426.

Van Oss, C., A. V. Panfilov, P. Hogeweg, F. Siegert and C. J. Weijer (181). Spatial pattern formation during aggregation of the slime mould *Dictyostelium discoideum*. *J. Theor. Biol.* 203–213.

Vasiev, B. and C. J. Weijer (1999). Modeling chemotactic cell sorting during *Dictyostelium discoideum* mound formation. *Biophys. J.* **76**, 595–605.

Vasiev, B. N., P. Hogeweg and A. V. Panfilov (1994). Simulation of *Dictyostelium discoideum* aggregation via reaction-diffusion model. *Phys. Rev. Lett.* **73**, 3173–3176.

Verkerke-Van Wijk, I. and P. Schaap (1997). cAMP, a signal for survival, in *Dictyostelium: A Model System for Cell and Developmental Biology*, Y. Maeda, K. Inouye and I. Takeuchi (Eds), Tokyo: Universal Academy Press, pp. 145–162.

Watts, D. J. and T. E. Treffry (1976). Culmination in the slime mould *Dictyostelium discoideum* studied with a scanning electron microscope. *J. Embryol. Exp. Morphol.* **35**, 323–333.

Weijer, C. J. (1999). The role of chemotactic cell movement in *Dictyostelium* morphogenesis, in *On Growth and Form: Spatio-temporal Pattern Formation in Biology*, Wiley Series in Mathematical and Computational Biology, M. A. J. Chaplain, G. D. Singh and J. C. McLachlan (Eds), Chichester: John Wiley & Sons, pp. 173–199.

Whittingham, W. F. and K. B. Raper (1960). Non-viability of stalk cells in *Dictyostelium*. *Proc. Natl. Acad. Sci. U.S.A.* **46**, 642–649.

Wilkins, M. R. and K. L. Williams (1995). The extracellular matrix of the *Dictyostelium discoideum* slug. *Experientia* **51**, 1189–1196.

Williams, G. B., E. M. Elder and M. Sussman (1984). Modulation of the cAMP relay in *Dictyostelium discoideum* by ammonia and other metabolites: possible morphogenetic consequences. *Dev. Biol.* **105**, 377–388.

Williams, J. (1997). Prestalk and stalk cell heterogeneity in *Dictyostelium*, in *Dictyostelium: a Model System for Cell and Developmental Biology*, Y. Maeda, K. Inouye and I. Takeuchi (Eds), Tokyo: Universal Academy Press, pp. 293–304.

Williams, J., N. Hopper, A. Early, D. Traynor, A. Harwood, T. Abe, M. N. Simon and M. Véron (1993). Interacting signalling pathways regulating prestalk cell differentiation and movement during the morphogenesis of *Dictyostelium*. *Development* **Suppl**, 1–7.

Williams, J. G., K. A. Jermyn and K. T. Duffy (1989). Formation and anatomy of the prestalk zone of *Dictyostelium*. *Development* **Suppl**, 91–97.

Zeeman, E. C. (1977). Slime mold culmination, in *Catastrophe Theory: Selected Papers*, Reading, MA: Addison-Wesley, pp. 216–233.

Received 29 May 2001 and accepted 13 November 2001